

USING AND MODELIZATION OF THE LAW OF ENERGY UNDER THE PATHOLOGY OF BLOOD FLOW IN THE CONSTRUCTION OF ELASTIC VARIABLE MODELS FOR BLOOD VESSEL WALLS

Dilafruz Shukrullaevna Nurjabova

Tashkent University of Information Technologies Karshi branch "Software Engineering"
dilyaranur1986@gmail.com

Sojida Rayimberdi qizi Ochilova

Tashkent University of Information Technologies Karshi branch
"Information Technologies"

ABSTRACT:

This article describes a mathematical model of the circulatory system for the cardiovascular system and provides a basic framework for the mathematical representation of cumulative medical parameters such as total vascular area, blood volume, self-regulation, and effects on the upper and inner heart. In mathematical terms, linear dependencies, differential, integral and differential equations are used.

Keywords: linear dependence, integral-differential equations, logical-dynamic equations, general vascular zone, self-regulation, influence on the upper and working heart, medical parameters.

INTRODUCTION:

The tone of the mathematical model of the degree of relation to the cardiovascular system and the circulatory system, which is related to time, is considered in the form of several specific areas of the cardiovascular system. When the experimental results, which reflect the volume tone and fluid dependence (blood fluidity), pressure and heart rhythm are reflected in the myocardial characteristics (in chronotope relations, dependence on velocity), the relationship between phases is shortened and weakened.

METHODS:

Consider the problem of blood flow in one vessel l cm long.

Both [1], we set the value of the model energy for this vessel as follows:

$$\varepsilon_{1D}(t) = \frac{\rho}{2} \int_0^l S \bar{u}^2 dx + \rho c^2 \int_0^l \int_0^S f(S) ds dx.$$

The first term corresponds to the kinetic energy of the liquid, and the second to the potential. For $f(S)$ (1.4), the second term on the right-hand side is always positive, therefore $\varepsilon_{1D}(t)$ is positive for any $t > 0$. We have

Lemma 1.1.1. For the system of equations (1.1) (recall that $\phi = 0$), supplemented by the equation of state (1.3), the following energy equality is true:

$$\frac{d}{dt} \varepsilon_{1D}(t) - \rho \int_0^l S \psi(t, x, S, \bar{u}) \bar{u} dx + S \bar{u} \left(\bar{p} + \frac{\rho}{2} \bar{u}^2 \right) \Big|_0^l = 0. \quad (1.18)$$

The proof of the lemma for the global blood circulation model written in the variables S and Q (1.15) can be found in [2,3]. Using the idea of this proof, we carry it out for our model (1.1).

Evidence. We multiply the second equation of system (1.1) by the product $\rho u S^-$ and integrate on the interval $(0, l)$:

$$\rho \int_0^l \bar{u} S \frac{\partial \bar{u}}{\partial t} dx + \rho \int_0^l \bar{u} S \frac{\partial (\bar{u}^2/2)}{\partial x} dx + \int_0^l \bar{u} S \frac{\partial \bar{p}}{\partial x} dx = \rho \int_0^l \bar{u} S \psi(t, x, S, \bar{u}) dx \quad (1.19)$$

We transform each term in the resulting equality (1.19) separately.

First term:

$$I_1 = \rho \int_0^l \bar{u} S \frac{\partial \bar{u}}{\partial t} dx = \rho \int_0^l S \frac{\partial (\bar{u}^2 / 2)}{\partial t} dx = \rho \frac{d}{dt} \int_0^l S \frac{\bar{u}^2}{2} dx - \frac{\rho}{2} \int_0^l \bar{u}^2 \frac{\partial S}{\partial t} dx.$$

Second term:

$$I_2 = \rho \int_0^l \bar{u} S \frac{\partial (\bar{u}^2 / 2)}{\partial x} dx = \frac{\rho}{2} S \bar{u}^3 \Big|_0^l - \rho \int_0^l \frac{\partial (S \bar{u}) \bar{u}^2}{\partial t} dx =$$

$$\frac{\rho}{2} S \bar{u}^3 \Big|_0^l + \rho \int_0^l \frac{\partial S \bar{u}^2}{\partial t} dx.$$

The last transition was carried out using the first equation system (1.1) under the assumption that $\varphi(t, x, S, \bar{u}) = 0$

Third term:

$$I_3 = \int_0^l \bar{u} S \frac{\partial \bar{p}}{\partial x} dx = \bar{p} S \bar{u} \Big|_0^l - \int_0^l \bar{p} \frac{\partial (S \bar{u})}{\partial x} dx.$$

Using expression (1.20), as well as equation of state (1.3), we continue the transformation:

$$I_3 = \bar{p} S \bar{u} \Big|_0^l - \bar{p} \frac{\partial S}{\partial t} dx = \bar{p} S \bar{u} \Big|_0^l + \frac{d}{dt} \int_0^l \int_S \bar{p} dx =$$

$$= \bar{p} S \bar{u} \Big|_0^l + p c_0^2 \frac{d}{dt} \int_0^l \int_S f(S) dx$$

Summing up I_1, I_2, I_3 , we obtain expression (1.18).

If the function $\psi(t, x, S, \bar{u})$ defines viscous friction (1.2), $R dx$ on the left-hand side of (1.18)

$$\int_0^l S \psi(t, x, S, \bar{u}) \bar{u} dx$$

(0) is negative. Thus, under homogeneous boundary conditions (1.10) at the points $x = 0$ and $x = l$, energy dissipation occurs in the global circulation model:

$$\frac{d}{dt} \varepsilon_{1D}(t) < 0.$$

The implementation of the global circulation model presented above, used in this work, was proposed and described in the article [4]. To solve the system of equations (1.1), grid-characteristic methods are used [5]: first-order

monotonic schemes and a hybrid scheme corresponding to the most accurate first-order monotonic scheme and the least oscillating second-order accurate scheme.

Let the global blood flow problem be calculated up to the n -th moment of time. To find a solution to the system of equations (1.1) in a given vessel with M design points and grid size h at the $(n + 1)$ th time step equal to τ , we use the following two-layer conservative difference scheme:

$$(V_m^{n+1} + V_m^n) / \tau + (F_{m+1/2}^{n+1/2} - F_{m-1/2}^{n+1/2}) / h = g_m^{n+1/2}. \quad (1.21)$$

Choosing a first-order interpolation formula for

calculation, $F_{m \pm 1/2}^{n+1/2}$

we get:

$$V_m^{n+1} = V_m^n + \tau (F_{m+1}^n - F_{m-1}^n) / 2h +$$

$$+ \tau \left[(\Omega^{-1} |\Lambda| \Omega)_{m+1/2}^n (V_{m+1}^n - V_m^n) - (\Omega^{-1} |\Lambda| \Omega)_{m+1/2}^n (V_{m+1}^n - V_{m-1}^n) \right] / 2h,$$

where Ω is a matrix whose rows are left eigenvectors (1.8); Λ is a diagonal matrix of eigenvalues (1.7).

The presented scheme is further used in numerical experiments. It has the minimum approximating viscosity under the stability condition on the class of explicit two-layer schemes of the first order of accuracy by positive approximation (1.5) [5]:

$$\sigma = \tau_{n+1} \max_{i,m} |(\lambda_i)_{i,m}^n| h \leq 1.$$

When calculating the global blood flow, the time step is variable and is determined by the formula:

$$\tau_{n+1} = \frac{0.9}{s_{\max}^n},$$

where $s_{\max}^n = \max_{k,i,m} |(\lambda_{ik})_{i,m}^n| h_k$, belongs to the set of indices of all vessels the network in question.

where the coefficients) $\alpha_1^n, \beta_1^n (\alpha_2^n, \beta_2^n)$ are calculated from the values at the points $M, M-1$ (1,2) from the previous time step.

$$\omega_{2,n}^M \left(\frac{V_M^{n+1} - V_M^n}{\tau} + \lambda_{2,n}^M \frac{V_M^n - V_{M-1}^n}{h} \right) = \omega_{2,n}^M g_M^n,$$

$$\omega_{1,n}^1 \left(\frac{V_1^{n+1} - V_1^n}{\tau} + \lambda_{1,n}^1 \frac{V_2^n - V_1^n}{h} \right) = \omega_{1,n}^1 g_1^n, \quad \text{or}$$

$$S_M^{n+1} = \alpha_1^n + \beta_1^n u_M^{n+1}, \quad (1.23)$$

$$S_1^{n+1} = \alpha_2^n + \beta_2^n u_1^{n+1}, \quad (1.24)$$

After discretization of the boundary conditions (1.11), (1.12) and (1.6), at each point of junction of the vessels, it is necessary to solve a system of nonlinear equations. For this, Newton's method is used. Numerical experiments have shown that Newton's method converges in a wide range of physiologically admissible parameters (different diameters, elastic properties of abutting vessels; different velocities and pressures) [6]. By identical transformations the dimension of the system can be halved:

$$F(S) = \Delta f + RP = 0, \quad (1.25)$$

$$f = \left\{ \varepsilon_{k_m} \left(\alpha_{k_m} S_{k_m} + \beta_{k_m} \right) S_{k_m} \right\}_{m=1}^M, P = \left\{ p_{k_m} \right\}_{m=1}^M$$

Where

$$R = \left\{ R_{ij} \right\}_{i,j=1}^M, R_{ij} = - \sum_{\substack{j=1 \\ j \neq i}}^M \prod_{\substack{m=1 \\ m \neq i}}^M R_{k_m}^j, R_{ij} = \prod_{\substack{m=1 \\ m \neq i}}^M R_{k_m}^j, \Delta = \det R = \sum_{i=1}^M \prod_{\substack{j=1 \\ j \neq i}}^M R_{k_m}^j,$$

R is a symmetric matrix that determines the hydraulic resistance for flows between vessels joining at a node, α_{km} , β_{km} are coefficients obtained by discretizing the compatibility condition for system (1.1) at the current time step, M is the number of vessels joining at a node, k_m is an index m- th vessel. Values from the previous time step are used as an initial approximation of the iterative process. Computational experiments have shown that such a choice of the initial approximation ensures the stable operation of the method.

To investigate the quality of convergence of Newton's method in this problem, a series of computational tests was carried out on the vessels of the systemic circulation. The vascular system was represented by two overlapping graphs corresponding to the venous and arterial parts. Both networks consisted of 341 edges and 335 vertices. Docking of veins and arteries was performed in 162 multinodules. At each node (multinode), the system (1.25) described above was solved by Newton's method. Several types of nodes were considered, differing in the number of incoming / outgoing ribs, their properties and blood flow intensity: the junction points of three vessels of the same or similar diameters (for example, 0.7 cm), but with different peak blood velocity in them (1-2 cm / s, 30 -40 cm / s, 80-90 cm / s); junction points of three vessels of different diameters (for example, 1.8, 1.7 and 1 cm); the points of joining of four vessels with different diameters (for example, 1.4, 1.4, 0.7 and 0.7 cm). We also studied the points of junction of veins and arteries, that is, vessels with different elastic properties ($c_0 = 700$ cm / s and $c_0 = 350$ cm / s for the analytical form of the equation of state (1.3)). The elastic properties of the vessel wall were described both using analytical approximation (1.3) and using fiber and spring-fiber models that reproduce the response of the wall of both a healthy vessel and in the presence of atherosclerotic plaques of various types or an installed cava filter (see the following sections and also [7-8]). In all these cases, Newton's method converged in 2-4 iterations with a given absolute accuracy of 10^{-6} , in 3-4 iterations with an accuracy of 10^{-8} to 10^{-12} . The most significant effect on the number of iterations required to achieve a given accuracy is exerted by the value of the velocity in the adjacent vessels. By changing the function ϕ on the right-hand side of the mass conservation law (1.1), one can take into account blood loss and wall

injuries. If the wound is punctate, it is assumed, for example, the following expression [7]:

$$\phi = -\alpha S,$$

where α is the point coefficient of blood loss intensity. The influence of various external forces can be taken into account by changing the function ψ in the law of conservation of momentum (1.1). Gravity, for example, in the simplest case is given by the formula [5]

$$\psi = G\rho\cos\alpha,$$

where G is the gravitational constant, α is the angle between the axis of the vessel and the direction of the free fall vector. Vibration effects of high intensity originating from traffic in megacities, at work, etc. can cause disturbances in the work of the cardiovascular system and change the picture of blood flow. Their influence can be described not only by changing the equations of the system, but also using a model of air movement in the lungs, taking into account gas exchange [3].

The work of muscles as a muscle pump can be taken into account by changing the equation of state:

$$\bar{p} = \rho c_0^2 f(S) + P_{add}(t).$$

$P_{add}(t)$ is some function that simulates muscle contractions. Changes in vascular stiffness c_0 in certain situations simulates the processes of auto regulation. Since everything in the body is interconnected, cardiovascular activity is affected by other physiological systems, various organs and tissues. When creating a graph of vessels, you can specify the type of each vertex [4]:

1. branch node;
2. fabric;
3. organ.

In the first case, the previously described conditions (1.11) - (1.12) are used to join the solutions. The tissues are characterized by an extensive capillary network. Here, the size of blood particles is comparable to the size of blood vessels, and we can assume that blood

flow is similar to the process of filtration of liquid through a porous medium, which obeys Darcy's law. For matching solutions at such a vertex, conditions (1.11) - (1.12) with suitable drag coefficients are also suitable, although more complex models can also be used, for example, [8]. To take into account the influence of the work of various organs on hemodynamics, the corresponding models are connected. An example of using the simplest kidney model is presented in [4]. This organ plays an important role in regulatory mechanisms.

RESULTS:

To achieve the goal, the following results are expected:

1. In this area it is associated with the development of mathematical models and methods for the numerical simulation of blood flow for specific patients. In this regard, it is extremely important to require the use of parameters measured by regular diagnostic methods.
2. To create software in this area based on non-invasively measured data is of great practical importance in cardiology when analyzing indications for coronary artery stenting, since it avoids expensive intravascular intervention and provides fundamentally new opportunities for virtual analysis.

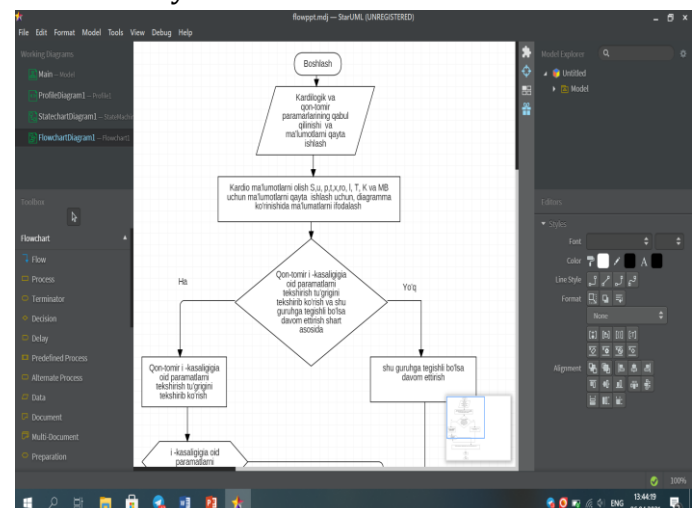


Fig1.1. Algorithm of app via UML

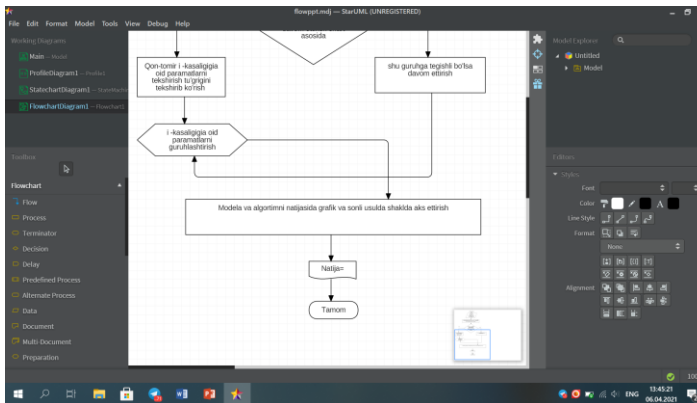


Fig1.2. Algorithm of app via UML

CONCLUSION:

The described approach to constructing a numerical implementation makes it possible to divide the problem into independent blocks for calculating the flow in each vessel and at each point of their docking. Although the described quasi-one-dimensional model of global circulation provides only averaged characteristics of blood flow, it is quite convenient to use, since it does not require large computational costs and, generally speaking, allows real-time calculations on computers with sufficient performance. Another regulatory mechanism is carried out by the nervous system. Baroreceptors are located at certain points of the vessel walls. With an increase in pressure, the activity of these baroreceptors increases and impulses transmitted to the brain and other parts of the central nervous system cause a decrease in the strength and heart rate, a change in the number of capillaries filled with blood, an increase in the stiffness and cross-section of the precapillary vessels (that is, a decrease in peripheral resistance). Assuming that the response to baroreceptor impulses occurs instantly, in practice, neural regulation can be implemented as follows [4]. A point is fixed at which constant pressure is required. With its increase or decrease, the length of the cardiac cycle changes, as well as the speed of propagation of the pulse wave and the resistance in the given vessels.

REFERENCES:

- 1) Kholodov A. C., Simakov C. C. Numerical study of the oxygen content in human blood at low-frequency influences // *Mathematical modeling*. 2008.Vol. 20 (4). S. 87-102.
- 2) Kholodov A. C. Some dynamic models of external respiration and blood circulation, taking into account their connectivity and transport of substances// *Computer models and progress of medicine* / Ed. Belotserkovsky O. M., Kholodova A.S. Moscow: Nauka, 2001, pp. 127-163
- 3) *Physiology of blood circulation: physiology of the vascular system* / Edited by BL Tkachenko: Science, 1984.
- 4) Dyachenko A.I., Shabelkov V.G. Shabel'kov V. *Mathematical models of the action of gravity on lung function*. Moscow: Nauka, 1985.
- 5) Koshelev V.B., Mukhin S.I., Sosnin N.V., Favorsky A.P. *Mathematical models of quasi-one-dimensional hemodynamics*. M.: MAKSPress, 2010.
- 6) Sherwin S. J., Franke V., Peiro J., Parker K. One-dimensional modeling of vascular network in space-time variables // *J. of Engineering Mathematics*. 2003.V. 47. P. 217-250.
- 7) E. Faggiano, A. Antiga, G. Puppini, A. Quarteroni, G.B. Luciani, and C Vergara. Helical flows and asymmetry of blood jet in dilated ascending aorta with normally functioning bicuspid valve. *Biomechanics and Modeling in Mechanobiology*, 4 (12): 801-813, 2013.
- 8) E. Faggiano, T. Lorenzi, and A. Quarteroni. Metal artefact reduction in computed tomography images by a fourth-order total variation flow. *Computer Methods in Biomechanics and Biomedical Engineering: Imaging & Visualization*, 3-4 (4): 202-213, 20.